Calibration of electron spectrometer resolution in attosecond streak camera

Ximao Feng, Steve Gilbertson, Sabih D. Khan, Michael Chini, Yi Wu, Kevin Carnes, and Zenghu Chang*

J. R. Macdonald Laboratory, Department of Physics, Kansas State University, Manhattan, KS 66506, USA
**chang@phys.ksu.edu*

Abstract: We report a new method for determining the energy resolution of time-of-flight spectrometers for detecting photoelectrons produced with attosecond XUV pulses. By measuring the width of the 2*s*2*p* autoionization line of helium, we found the resolution of our spectrometer to be ~0.6 eV for electrons at 35.5 eV. Furthermore, the resolution in the 10 to 35 eV range was determined by applying a retarding potential at the entrance of the drift tube.

OCIS codes: (320.7090) Ultrafast optics: Ultrafast lasers; (020.2649) Atomic and molecular physics: Strong field laser physics.

References and links

1. M. Hentschel, R. Kienberger, C. Spielmann, G. A. Reider, N. Milosevic, T. Brabec, P. Corkum, U. Heinzmann, M. Drescher, and F. Krausz, "Attosecond metrology," Nature **414**(6863), 509–513 (2001).
2. X. Feng, S. Gilbertson, H. Mashiko, H. Wang, S. D. Khan, M. Chini, Y. Wu, K. Zhao, and Z. Chang, "Generation of isolated attosecond pulses with 20 to 28 femtosecond lasers," Phys. Rev. Lett. **103**(18), 183901 (2009).
3. S. Gilbertson, X. Feng, S. D. Khan, M. Chini, H. Wang, H. Mashiko, and Z. Chang, "Direct measurement of an electric field in femtosecond Bessel-Gaussian beams," Opt. Lett. **34**(16), 2390–2392 (2009).
4. Y. Mairesse, and F. Quéré, "Frequencyresolved optical gating for complete reconstruction of attosecond bursts," Phys. Rev. A **71**(1), 011401 (2005).
5. Z. Chang, "Controlling attosecond pulse generation with a double optical gating," Phys. Rev. A **76**(5), 043802 (2007).
6. M. Chini, H. Wang, S. D. Khan, S. Chen, and Z. Chang, "Retrieval of satellite pulses of single isolated attosecond pulses," Appl. Phys. Lett. **94**(16), 161112 (2009).
7. K. T. Kim, K. S. Kang, M. N. Park, T. Imran, G. Umesh, and C. H. Nam, "Comparison of RABITT and FROG measurements in the temporal characterization of attosecond pulse trains," ArXiv eprints: 0707.4228 (2007).
8. U. Fano, and J. Cooper, "Line profiles in the faruv absorption spectra of the rare gases," Phys. Rev. **137**(5A), A1364–A1379 (1965).
9. R. P. Madden, D. L. Ederer, and K. Codling, "Instrumental aspects of synchrotron xuv spectroscopy," Appl. Opt. **6**(1), 31 (1967).
10. H. D. Morgan, and D. L. Ederer, "Photoionization cross section of helium for photon energies 5967 eV: The $(sp,2n^+)$ $^1P^0$ Rydberg series of autoionizing resonances," Phys. Rev. A **29**(4), 1901–1906 (1984).
11. H. Mashiko, S. Gilbertson, C. Li, S. D. Khan, M. M. Shakya, E. Moon, and Z. Chang, "Double optical gating of high-order harmonic generation with carrier-envelope phase stabilized lasers," Phys. Rev. Lett. **100**(10), 103906 (2008).
12. Y. Oishi, M. Kaku, A. Suda, F. Kannari, and K. Midorikawa, "Generation of extreme ultraviolet continuum radiation driven by a sub-10-fs two-color field," Opt. Express **14**(16), 7230–7237 (2006).
13. P. B. Corkum, N. H. Burnett, and M. Y. Ivanov, "Subfemtosecond pulses," Opt. Lett. **19**(22), 1870 (1994).
14. O. Tcherbakoff, E. Mevel, D. Descamps, J. Plumridge, and E. Constant, "Timegated highorder harmonic generation," Phys. Rev. A **68**(4), 043804 (2003).
15. Z. Chang, "Single attosecond pulse and xuv supercontinuum in the highorder harmonic plateau," Phys. Rev. A **70**(4), 043802 (2004).
16. H. Mashiko, S. Gilbertson, M. Chini, X. Feng, C. Yun, H. Wang, S. D. Khan, S. Chen, and Z. Chang, "Extreme ultraviolet supercontinua supporting pulse durations of less than one atomic unit of time," Opt. Lett. **34**(21), 3337–3339 (2009).
17. S. Gilbertson, H. Mashiko, C. Li, S. D. Khan, M. M. Shakya, E. Moon, and Z. Chang, "A lowloss, robust setup for double optical gating of high harmonic generation," Appl. Phys. Lett. **92**(7), 071109 (2008).

#120435 - $15.00 USD Received 24 Nov 2009; revised 30 Dec 2009; accepted 1 Jan 2010; published 12 Jan 2010

18. S. J. Brotton, S. Cvejanovic, F. J. Currell, N. J. Bowring, and F. H. Read, "Electron-impact excitation of the doubly excited states of helium below the N=3 He^+ threshold," Phys. Rev. A **55**(1), 318–328 (1997).
19. X. Liu, Y. Huang, L. Zhu, Z. Yuan, W. Li, and K. Xu, "Numerical determination of profile parameters for fano resonance with definite energy resolution," Nucl. Instrum. Methods Phys. Res. A **508**(3), 448–453 (2003).
20. K. Pearson, "Contributions to the mathematical theory of evolution. ii. Skew variation in homogeneous material," Philos. Trans. R. Soc. Lond. A **186**(-1), 343–414 (1895).

1. Introduction

Single isolated extreme ultraviolet (XUV) attosecond pulses are important tools for studying electron dynamics with pump-probe methods. Attosecond streak cameras have been used to characterize and utilize such pulses [1–3]. To characterize isolated attosecond pulses, both the XUV pulses and femtosecond near infrared (NIR) laser pulses are focused onto a detection gas target where they overlap temporally and spatially. The XUV pulses free electrons from the atoms through single photon ionization, which produces an attosecond electron replica of the attosecond XUV pulses. The strong NIR field gives a momentum shift to the electrons, which is called attosecond streaking. The electron energy change depends on the delay between the XUV pulse and NIR field. A spectrogram is formed when a series of electron spectra with different XUV-NIR delays are collected, from which the XUV pulse parameters are retrieved with a method called FROG-CRAB [4]. Time-of-flight (TOF) spectrometers have been used in attosecond streak cameras. At each time delay, the TOF spectrometer collects the whole spectrum of the photoelectrons that covers tens of electron volts at one time with high efficiency, which is important because the electron count rate is usually low due to the limited XUV flux.

A single isolated attosecond pulse can be extracted from a pulse train with different gating techniques. The main pulses are accompanied by weaker "satellite" pulses regardless of the gating scheme used. Experimentally, these satellite pulses are evident by the amplitude modulation in photoelectron spectra. Therefore, for an accurate characterization of the satellite pulse contrast, the energy resolution of the TOF spectrometer must be sufficiently high. The requirement on the energy resolution depends on the time spacing between the main pulse and the adjacent satellite pulses. The spacing can be half of an optical cycle of the driving laser when the fundamental laser field is used alone in the gating, or it can be a full laser period when the second harmonic field is added to the driving laser such as in the case of double optical gating (DOG) [5]. Here we only consider the latter case. For the Ti:Sapphire laser working at 800 nm, one cycle is 2.7 fs or in photon energy, the period of the corresponding spectral modulation is 1.55 eV. Figure 1 shows the satellite pulse contrast retrieved for the full-cycle periodicity case from the FROG-CRAB method with simulated noise-free data, as a function of the spectrometer energy resolution [6]. The results show that the required resolution in the whole energy range should be better than 0.8 eV if the retrieved satellite pulse contrast is within one order of magnitude deviation from the real value.

The electron spectrometers at synchrotron facilities are calibrated by setting the x-ray source to a very narrow and known bandwidth with monochromators. The main difficulty of calibration of the TOF electron spectrometers in attosecond streak cameras is that it is hard to find an XUV light source with a known linewidth comparable to the resolution of the spectrometer. Kim *et al.* measured their spectrometer resolution from the photolines of helium atoms with the neon III plasma emission [7]. However, that method can only determine the spectrometer resolution on the low energy side (less than 1 eV). To calibrate the electron spectrometer resolution *in situ* over a broad energy range, we propose and demonstrate a new method by measuring the autoionization linewidth after double excitation in helium. We also show that by applying retarding potentials, we can calibrate the energy resolution of the spectrometer in the energy range of interest.

#120435 - $15.00 USD Received 24 Nov 2009; revised 30 Dec 2009; accepted 1 Jan 2010; published 12 Jan 2010

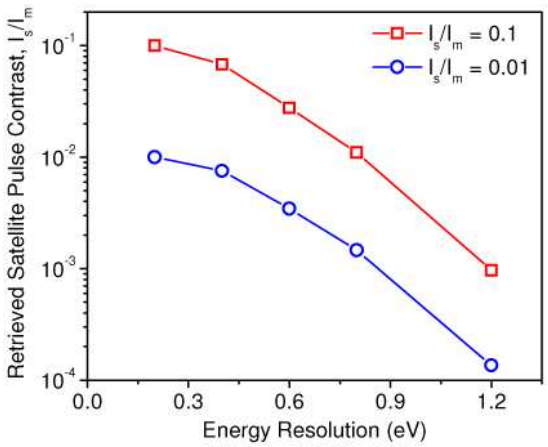

Fig. 1. Dependence of the retrieved satellite pulse amplitude on the energy resolution of the electron spectrometer. Only one satellite pulse a laser cycle away from the main pulse is included. I_m and I_s are the intensities of the main pulse and satellite pulse respectively.

2. Experimental setup

The origin of the Fano peak at 60.1 eV is well understood. When a helium atom absorbs an XUV photon, two quantum mechanical processes can happen: direct photoionization of one 1*s* electron, and double excitation. In the double excitation, both 1*s* electrons are excited to the 2*s*2*p* state. Then, one electron returns to the 1*s* state of He^+ whereas the other is freed through autoionization. These two channels interfere with each other leading to a sharp asymmetric peak with a linewidth of 38 meV at 35.5 eV in the electron spectrum, which is called the Fano profile [8–10]. Since the width of the Fano peak is much narrower than the TOF spectrometer resolution, it is suitable for measuring the energy resolution.

Our calibration method requires the generation of a pulsed XUV continuum around 60.1 eV. Such a light source can naturally exist in an attosecond streak camera because the spectrum of an isolated attosecond pulse is an XUV continuum. Consequently, this approach allows *in situ* calibration of the TOF spectrometer resolution. In our streak camera, the attosecond XUV continuum is generated by double optical gating (DOG) [11], which is a combination of two-color gating [12] and polarization gating [13–15]. The laser field for DOG is elliptically polarized on the leading and trailing edges of the pulse. Only the central part with small ellipticity generates attosecond pulses, thus forming a temporal gate [15]. If the gate width is smaller than the spacing between two neighboring attosecond pulses, a single attosecond pulse is extracted. With DOG, XUV supercontinua covering the photon energy range from 30 to 600 eV have been generated [16].

The setup for determining the resolution of the TOF electron spectrometer with a position sensitive delay line detector is sketched in Fig. 2, which is a subset of our attosecond streak camera (the NIR streaking laser beam is not shown) [2]. The required XUV spectrum was obtained with double optical gating using 8 fs NIR lasers. The laser pulses were produced with a hollow-core fiber and chirped mirrors by compressing 30 fs pulses from a chirped pulse amplifier at a 1.5 kHz repetition rate. The NIR laser field was transformed into a field with the required time-dependent ellipticity for DOG when passed through two quartz waveplates and a type I phase-matched barium borate (BBO) crystal [17]. Then, the laser beam was focused onto a neon gas cell to generate the XUV continuum. Finally, the XUV beam was focused onto a helium gas jet by a broadband multilayer Mo/Si mirror which has 6% reflectance around 60 eV. The freed electrons were detected by the TOF electron spectrometer with a position sensitive delay line detector.

#120435 - $15.00 USD Received 24 Nov 2009; revised 30 Dec 2009; accepted 1 Jan 2010; published 12 Jan 2010

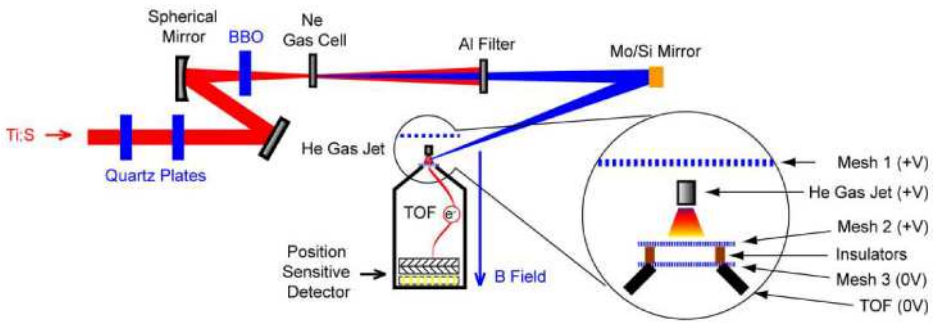

Fig. 2. Schematic of the experimental setup for calibrating the TOF electron spectrometer with position sensitive delay line detector. The retarding system was magnified to show the details.

Attosecond XUV pulses corresponding to a smooth continuous XUV spectrum extending up to 65 eV were generated in the first neon gas cell. When such XUV light was absorbed by the helium gas in front of the TOF spectrometer to be calibrated, a photoelectron pulse was produced. Due to the Fano resonance at 60.1 eV photon energy, the spectrum of the electron pulse consists of a sharp peak with 38 meV width at 35.5 eV sitting on a continuum [8–10]. The Fano peak was used for determining the energy resolution of our electron spectrometer. To characterize the energy resolution over a range of electron energy, we installed a simple retarding potential system to slow down the electrons. The system, as shown in Fig. 2, is composed of three meshes. Meshes 1 and 2 were given the same positive potentials (+V) as the helium gas jet so that the space between the two meshes can be approximated to be electric field free. Mesh 3 is conductively connected to the cone of the detector chamber, and is insulated from Mesh 2 by an insulator 0.5 mm thick. The potential difference between Meshes 2 and 3 decelerates the electrons when they fly to the detector.

A pair of Helmholtz coils provided a uniform magnetic field (about 1.1 gauss) along the axis of the TOF, the z direction, covering over the whole 295 mm electron flight region. Two pairs of ribbon coils were used to cancel the x and y components of the earth's magnetic field. The delay line detector (RoentDek, DLD120) is composed of two multi-channel plates (MCPs) in a Chevron configuration and two layers of anode wires that are wound along the x and y directions. The combination of signals from the MCP and the delay lines give the time and position of electrons when hitting the detector. The signals were digitized using a combination of a multi-channel constant fraction discriminator (Phillips Scientific, Model 715) and a 16-channel multi-hit TDC (CAEN, V1290N).

There are several advantages of using a large area position sensitive detector (120 mm in diameter), and the uniform magnetic field along the spectrometer axis. First, the acceptance angle is large, ±13 degrees for 45 eV electrons and ±23 degrees for 10 eV electrons, which is important for increasing the count rate. Second, compared to a MCP-only detector, a delay-line detector can improve the energy resolution, using the additional position information, when the acceptance angle is large. Third, momentum of the electron, not just energy, is measured. Finally, it is easy to implement differential pumping, i.e, adding a cone with a small opening (1 mm diameter in our case) so that high gas density can be delivered to the detection region without affecting the MCP operation.

When the energy resolution of the TOF spectrometer is limited by the time resolution of the detector and electronics, the most straightforward way to improve the resolution of the spectrometer is to extend the electron flight distance. However, for the current design with magnetic field, there is a limit on the flight distance because of the "magnetic node." When an electron flies to the detector with energy, E, the wiggle spectrum, that is, the radial position versus the arrival time, t, can be written as:

#120435 - $15.00 USD Received 24 Nov 2009; revised 30 Dec 2009; accepted 1 Jan 2010; published 12 Jan 2010

$$r = \frac{2\sqrt{2m_e E - (m_e S/t)^2}}{eB}\left|\sin\left(\frac{eBt}{2m_e}\right)\right|, \qquad (1)$$

where m_e is the electron mass, e is the electron charge, S is the flight distance, and B is the magnetic field experienced by the electron. Figure 3 presents some wiggle spectra calculated with Eq. (1) for electrons with different energies. The horizontal dotted line shows the radial boundary of the detector, beyond which the electrons cannot be detected. From the figure, one can see that all the electrons hit the center of the detector with a cyclotron frequency $\omega = eB/m_e$. All electron trajectories, independent of their initial kinetic energies, cross at these magnetic nodes. On the energy spectrum, they form a series of "holes", where there is no energy information. To retrieve a single attosecond pulse, these "holes" must be avoided, and all the electrons of interest should be contained between two magnetic nodes. This sets a limit on the flight time and the flight length of the electrons. The current magnetic field of 1.1 gauss, which gives a node around 2.5 eV, is a compromise between the acceptance angle and the node position.

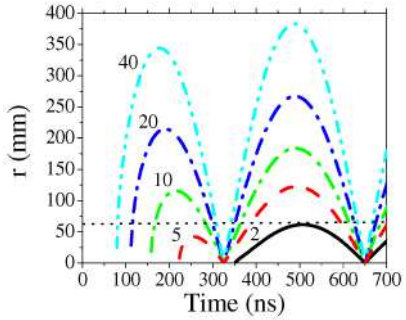

Fig. 3. Calculated radial position on the detector as a function of the time of flight for electrons of different energies when they arrive at the detector. The number beside each curve shows the kinetic energy (in eV) of the electron corresponding to that curve. In the calculation, the flight distance is 295 mm, and the magnetic field is 1.1 gauss. The horizontal dotted line represents the radius of the detector (60 mm).

3. Results and discussion

The photoelectron spectra from helium measured with different retarding potentials in the TOF are presented in Fig. 4. All other curves are shifted vertically with respect to the 0 volt spectrum for a clear presentation. The *2s2p* autoionization peak, sitting on a continuous photoelectron background originating from the direct photoionization channel, shifts from 35.5 eV when the retarding potential is 0, to 10.9 eV when the retarding potential is −30 V. The energy shifts of the peak are not equal to the corresponding applied retarding potentials. We attribute this difference to the lack of perfect uniform electric field due to the disturbance of the gas jet and/or the external stray electric field. The resulted effective retarding potential is around 80% of the actual one. The electron energy scale is calibrated with the high order harmonic peak positions generated from neon using linearly polarized 30 fs laser pulses. The Fano peak position measured with 0 V retarding potential, well-known at a photon energy of 60.1 eV, confirmed the energy calibration. The big bump near the high energy cutoff of the spectra results from the high reflectance of the multilayer Mo/Si mirror around 65 eV photon energy.

#120435 - $15.00 USD Received 24 Nov 2009; revised 30 Dec 2009; accepted 1 Jan 2010; published 12 Jan 2010

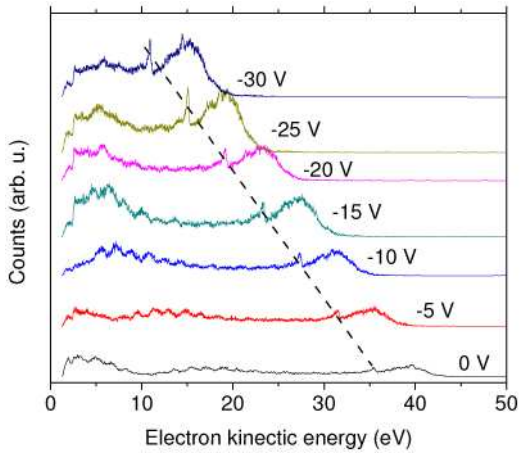

Fig. 4. Photoelectron energy spectra produced by absorbing isolated XUV attosecond pulses. The number beside each of the spectra shows the retarding potential added in collecting the corresponding spectrum. The dashed line connects all the autoionization peaks for guiding the eye.

The spectrometer resolution should be obtained by a deconvolution of the Fano profile and the measured results [18, 19]. However, our spectrometer resolution is at least five times wider than the width of the autoionization peak. Therefore, the contribution of the intrinsic Fano peak width to the measured peak width is neglected. We fitted the *2s2p* peak with a Pearson type IV function [20] and a nonlinear background. The full width at half maximum (FWHM) of the measured peak is defined as the energy resolution. As an example, Fig. 5 shows the fitting results for the spectrum when the retarding potential is –25 V. The FWHM of the Pearson function is 0.30 eV, and the peak position is at 15.1 eV.

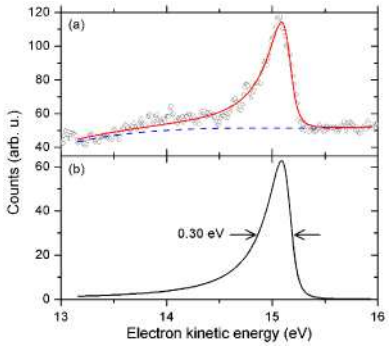

Fig. 5. Curve fitting with a Pearson type IV function and a cubic background for the experiment spectrum with retarding potential of –25 V. (a) Experimental data (empty circles), fit curve (red solid line), and cubic background (dashed line). (b) The resulted Pearson function, which is the difference between the fit curve and the cubic background in (a).

The TOF spectrometer energy resolution for electrons with different kinetic energies obtained from the fittings is plotted in Fig. 6 as the red line and empty circles. The resolution changes from 0.3 to 0.6 eV when the electron energy increases from 10 eV to 35 eV. Since the resolution is better than 0.8 eV, the contrast of main attosecond pulses to the satellite pulses can be measured within an uncertainty of one order of magnitude as discussed in the introduction, when the spectrum of the attosecond pulse is in the energy range of Fig. 6.

#120435 - $15.00 USD Received 24 Nov 2009; revised 30 Dec 2009; accepted 1 Jan 2010; published 12 Jan 2010

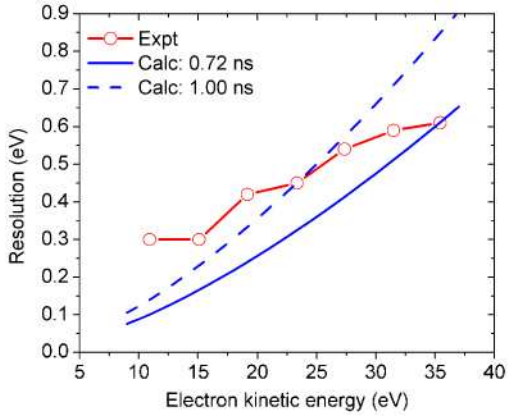

Fig. 6. Comparison of the spectrometer resolution as a function of the electron kinetic energy between the experimentally measured and the calculated values.

The significant improvement of energy resolution of the TOF spectrometer by adding the retarding potential is the evidence that the time resolution of the detection system is one of the dominating factors that limit the energy resolution. The contribution of the time resolution to the energy resolution was calculated using the well-known relation between the resolution of the spectrometer, ΔE, and the electron energy E:

$$\Delta E = \frac{2^{3/2}\Delta t}{m_e^{1/2} S} E^{3/2}, \tag{2}$$

where Δt is the total time resolution of the MCP detector and electronics which includes the amplifier, the constant fraction discriminator and the time-to-digital converter.

The calculated energy resolution as a function of the electron kinetic energy calculated with Eq. (2) is plotted in Fig. 6 for two different time resolutions: 0.72 ns (blue solid line) and 1 ns (blue dashed line). One can see that four of the experimental data points on the high energy side fall between these two curves. The deviation of the measured curve from the $E^{3/2}$ indicates that other factors such as the earth's magnetic field also contribute significantly to the energy resolution.

4. Conclusions

In conclusion, we demonstrated that the Fano resonance peak of helium is an excellent electron source for *in situ* calibration of the energy resolution of electron TOF spectrometers in attosecond streak camera setups. The electron spectrum with a sharp peak (38 meV) at 35.5 eV electron energy can be produced by ionizing helium atoms with the XUV continuum from the isolated attosecond pulse source that already exists in the streak camera. The resolution at other lower electron energies was measured by applying a retarding potential at the entrance of the TOF drift tube. Since there are a series of Fano peaks in helium, the method demonstrated here can be applied to calibrate energy resolutions higher than 35.5 eV using other Fano peaks.

Acknowledgements

This work is supported by the U. S. Army Research Office under Grant No. W911NF-07-1-0475, by the NSF under Grant No. 0457269, and by the Chemical Sciences, Geosciences, and Biosciences Division, U.S. Department of Energy.

#120435 - $15.00 USD Received 24 Nov 2009; revised 30 Dec 2009; accepted 1 Jan 2010; published 12 Jan 2010